^{2}H and ^{195}Pt NMR Studies of Molecular and Electron Spin Dynamics in Paramagnetic $[Cu(H_2O)_6][PtCl_6]$*

Takahiro Iijima, Kengo Orii, Motohiro Mizuno, and Masahiko Suhara

Department of Chemistry, Faculty of Science, Kanazawa University, Kanazawa 920-1192, Japan.

Z. Naturforsch. **53 a,** 447–452 (1998); received December 31, 1997

The temperature dependences of ^{2}H and ^{195}Pt NMR spectra and the spin-lattice relaxation time T_1 were measured for $[Cu(H_2O)_6][PtCl_6]$. From the simulation of ^{2}H NMR spectra, the jump rate of 180° flips of the water molecules (k), the nuclear quadrupole interaction parameters ($e^2Qq/h, \eta$) and the electron-nucleon dipolar interaction parameter (ν_D) were obtained. By measuring ^{2}H T_1, k was estimated in the temperature range where the spectrum is insensitive to the motion of the water molecules. Above the phase transition temperature, the pre-exponential factor $k_0 = 8\times10^{11}\,s^{-1}$ and the activation energy E_a=15 kJmol^{-1} for 180° flips of the water molecules were obtained from the spectral simulation and T_1. ^{195}Pt NMR spectra showed an axially symmetric and unsymmetric powder pattern of the chemical shift anisotropy at the high and low temperature phase, respectively. For the deuterated compound, the correlation times of the electron spin in Cu^{2+} were estimated from ^{195}Pt T_1 and the activation energy for jumping between the different configurations of Jahn-Teller distortion Δ = 200 K was obtained.

Introduction

$[Cu(H_2O)_6][PtCl_6]$ undergoes a phase transition caused by the cooperative Jahn-Teller effect at 135 K, and the transition temperature shifts to the lower side by 6 K on deuteration [1 - 3]. $[Cu(H_2O)_6]^{2+}$ ions, changing between the three Jahn-Teller distorted configurations by thermal excitation in the high temperature phase, distort to one of these configurations in the low temperature phase [1 - 5]. The lower temperature shift of the phase transition, however, cannot be explained by the change in the motion of $[Cu(H_2O)_6]^{2+}$ due to the mass difference between ^{1}H and ^{2}H, and detailed information about the H site is required for clarifying the nature of this phase transition.

Although ^{2}H NMR is effective to study the environment of the H site, the analysis of the powder spectra of the paramagnetic compound obtained by the usual quadrupole echo method is very difficult because of the dephasing due to the paramagnetic shift [6]. Recently, ^{2}H NMR spectra in paramagnetic compounds, using the shift-compensated pulse sequence which refocuses both the quadrupolar interaction and the paramagnetic shift, have been investigated [6 - 11]. From the analysis of the powder spectra obtained by this method, the jumping rate of the molecules, static nuclear quadrupolar interaction parameters and the paramagnetic shift parameter have been obtained [7, 8]. In the present work, in order to obtain information about the H site and the motion of H_2O molecules in $[Cu(H_2O)_6][PtCl_6]$, we measured ^{2}H NMR spectra of the powder sample using the shift compensated pulse sequence and performed a simulation. ^{2}H T_1 was measured to study the motion of H_2O in the temperature range where the spectrum is insensitive to the H_2O motion and the electron spin dynamics in Cu^{2+}. Moreover, the isotope effect on the phase transition is discussed from ^{195}Pt NMR spectra and T_1.

Experimental

The deuterated sample was obtained by repeated recrystallization from heavy water. ^{2}H and ^{195}Pt NMR spectra were measured using a CMX-300 spectrometer with a 5 mmø sample tube at 45.825 and 64.160 MHz, respectively. For ^{2}H NMR spectra, the

* Presented at the XIVth International Symposium on Nuclear Quadrupole Interactions, Pisa, Italy, July 20–25, 1997.

Reprint requests to Dr. M. Mizuno;
E-mail: mizuno@wriron1.s.kanazawa-u.ac.jp.

0932-0784 / 98 / 0600-0447 $ 06.00 © – Verlag der Zeitschrift für Naturforschung, D-72072 Tübingen

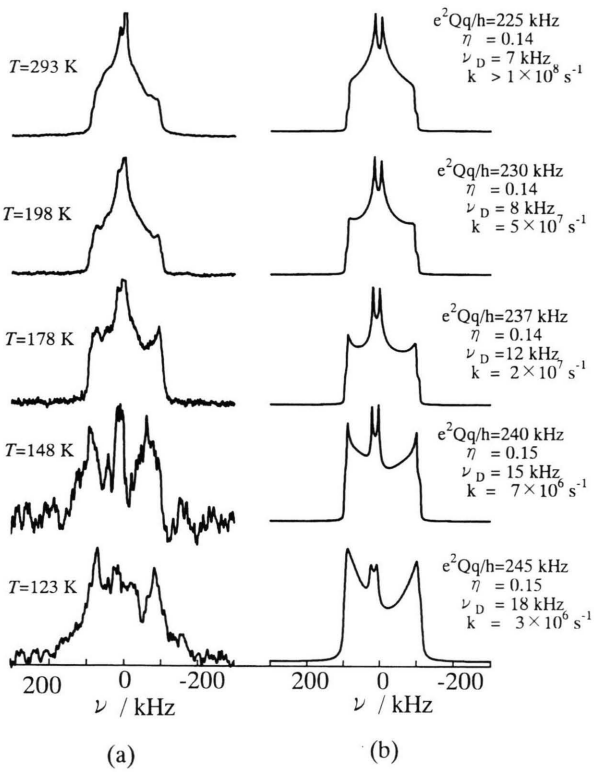

Fig. 1. Temperature dependence of ^2H NMR spectra in $[Cu(D_2O)_6][PtCl_6]$. (a) and (b) show the observed and the theoretical spectra, respectively.

$(\pi/2)_x$-τ/2-$(\pi)_y$-τ/2-$(\pi/2)_y$-τ/2-$(\pi)_y$-τ/2-acq pulse sequence was used, which refocuses the dephasing due to the quadrupolar interaction and the paramagnetic shift [6 - 11]. The $\pi/2$ pulse width and $\tau/2$ were 1.5 μs and 20 μs, respectively. The $(\pi/2)_x$-τ-$(\pi)_y$-τ-acq pulse sequence was used for the ^{195}Pt NMR spectra. ^2H and ^{195}Pt NMR T_1 were measured by the inversion recovery method.

Results and Discussion

^2H NMR

Figure 1(a) shows the temperature dependence of observed ^2H NMR spectra. The nuclear quadrupole interaction and the electron-nuclear dipole interaction between the ^2H nuclei and Cu^{2+} ions are considered to contribute mainly to the spectra. The spectral simulation was performed by using the two-site jump model of the water molecules for 180° flips about the HOH bisector which is assumed to be parallel to Cu-O bond.

For the ^2H-Cu^{2+} dipolar interaction, the contribution from the nearest Cu^{2+} ion ($\omega_D = 2\pi\nu_D$) was estimated. On the assumption of the isotropic g tensor, the site frequency ω_i is written by the second-order Wigner rotation matrix $D^{(2)*}_{nm}(\Omega)$ [8, 12, 13] as

$$\omega_i = \mp\omega_Q - \omega_P, \tag{1}$$

$$\omega_Q = \sqrt{\frac{3}{2}} \sum_{n,m=-2}^{2} D^{(2)*}_{0n}(\psi,\theta,\phi) D^{(2)*}_{nm}(\alpha,\beta,\gamma) T^{(2)}_{mQ}, \tag{2}$$

$$\omega_P = \sum_{n=-2}^{2} D^{(2)*}_{0n}(\psi,\theta,\phi) D^{(2)*}_{n0}(\alpha',\beta',\gamma') \omega_D, \tag{3}$$

$$T^{(2)}_{0Q} = \sqrt{\frac{3}{8}}\, e^2Qq/\hbar, \quad T^{(2)}_{\pm 2Q} = (\eta/2)e^2Qq/\hbar, \tag{4}$$

$$\omega_D = 2\gamma_D g \mu_B \langle \boldsymbol{S}_z \rangle r^{-3}, \tag{5}$$

where, (α,β,γ), (ψ,θ,ϕ) and (α',β',γ') represent the Euler angles for the transformation from the molecular axes to the principal axes system of the quadrupolar tensor, from the laboratory axes to the molecular axes and from the molecular axes to the principal axes system of the dipolar tensor between the ^2H nuclei and the nearest Cu^{2+}, respectively. $\langle \boldsymbol{S}_z \rangle$ is the expectation value of $\boldsymbol{S}_z$ of the unpaired electron spin in Cu^{2+}. γ_D is the gyromagnetic ratio of ^2H nucleus, μ_B the Bohr magneton. r is the distance between the ^2H nucleus and Cu^{2+}. The frequencies of ^2H in the two sites (ω_1,ω_2) were specified by $\alpha = \alpha' = 0$ and π. The positions of H atoms are not known, and we assumed $\gamma = 0$. The used angles between the rotation axis and the quadrupole principal axis $\beta = 55°$, and between the rotation axis and the Cu-H vector $\beta' = 17°$ were based on the crystal structure of $[Ni(H_2O)_6][SiF_6]$ [14, 15]. The signal which is collected beginning at the top of the resulting echo $G(t,\theta,\phi)$ is written as [8, 12]

$$G(t,\theta,\phi) = \boldsymbol{P} \cdot \exp[\hat{\boldsymbol{A}}t]\exp(\hat{\boldsymbol{A}}\tau)\exp(\hat{\boldsymbol{A}}^*\tau) \cdot \boldsymbol{1}, \tag{6}$$

$$\hat{\boldsymbol{A}} = \begin{pmatrix} i\omega_1 - k & k \\ k & i\omega_2 - k \end{pmatrix}, \tag{7}$$

$$\boldsymbol{P} = (P_1, P_2), \quad \boldsymbol{1} = (1,1). \tag{8}$$

Here, $\boldsymbol{P}$ is a vector of site populations and we assumed $P_1 = P_2 = 1/2$. The signal of the powder sample $G(t)$

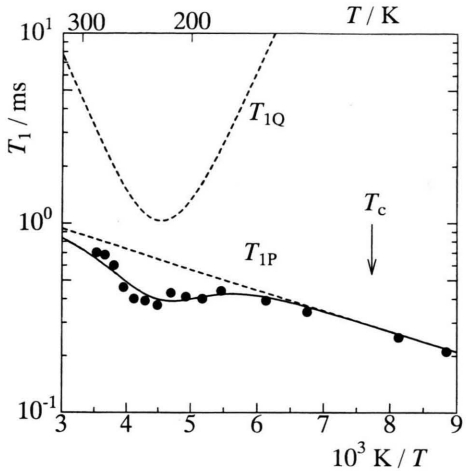

Fig. 2. Temperature dependence of ^2H NMR T_1 in $[Cu(D_2O)_6][PtCl_6]$. The broken lines show the theoretical curves of T_{1Q} and T_{1P}. The solid line shows the theoretical curve of T_1.

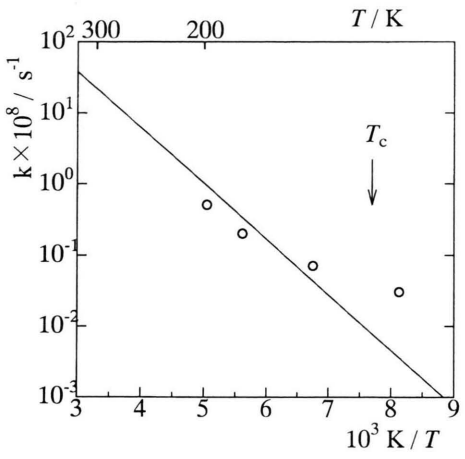

Fig. 3. Temperature dependence of the jumping rate (k) for the 180° flip of H_2O. The open circle shows k estimated from the spectral simulation and the solid line shows the theoretical curve with the parameters obtained by T_1 measurements.

is given by

$$G(t) = \int_0^{2\pi} \int_0^{\pi} G(t, \theta, \phi) \sin\theta d\theta d\phi. \quad (9)$$

The spectrum is obtained by the Fourier transform of $G(t)$. The theoretical spectra are shown in Figure 1(b). The jump rate of 180° flips of the water molecules (k), the nuclear quadrupole interaction parameters ($e^2Qq/h, \eta$) and the electron-nuclear dipole interaction parameter (ν_D) obtained by the fitting are shown on the right side of Figure 1(b). Because of the fast motion limit, the spectrum at 293 K was insensitive to the motion of H_2O, and k could not be determined accurately. For the quadrupole interaction parameters, though η was almost temperature independent, e^2Qq/h which showed 245 kHz at 123 K, decreased with increasing temperature and showed 225 kHz at 293 K. The observed decrease of e^2Qq/h can be considered to reveal the existence of rapid motions, other than the 180° flips of the water molecules, which average the electric field gradient at ^2H site.

Figure 2 shows the temperature dependence of ^2H T_1. The shallow minimum observed at ca. 230 K can be considered to be due to the fluctuation of the EFG at the ^2H nucleus caused by the 180° flips of the water molecules. At low temperatures, T_1 decreased gradually with decreasing temperature, and the relaxation can be considered to be dominated by the magnetic dipole interaction between ^2H nuclei and Cu^{2+} ions. The quadrupole relaxation rate (T_{1Q}^{-1}) caused by the 180° flips of the water molecules can be written by assuming $\eta = 0$ as [16, 17]

$$T_{1Q}^{-1} = \frac{1}{10}\left(\frac{3e^2Qq}{4\hbar}\right)^2 (\sin 2\beta)^2 \cdot \left\{\frac{\tau_c}{1+\omega_N^2\tau_c^2} + \frac{4\tau_c}{1+\omega_N^2\tau_c^2}\right\}, \quad (10)$$

where β is the angle between the rotation axis and the quadrupole principal axis, ω_N the angular NMR frequency and τ_c the correlation time for the 180° flips of the water molecules. Assuming Arrhenius relation, τ_c is given by

$$\tau_c = \tau_0 \exp(E_a/RT), \quad (11)$$

where, τ_0 and E_a are the correlation time at infinite temperature and the activation energy for the 180° flips of the water molecules. If the paramagnetic dipole relaxation is caused by the fluctuation of the electron spin in Cu^{2+}, the relaxation rate (T_{1P}^{-1}) can be written as [3, 18, 19]

$$T_{1P}^{-1} = \frac{2}{15}\gamma_D^2 g^2 \mu_B^2 \sum_i r_i^{-6} S(S+1) \cdot \left\{\frac{3\tau_e}{1+\omega_N^2\tau_e^2} + \frac{7\tau_e}{1+\omega_e^2\tau_e^2}\right\}, \quad (12)$$

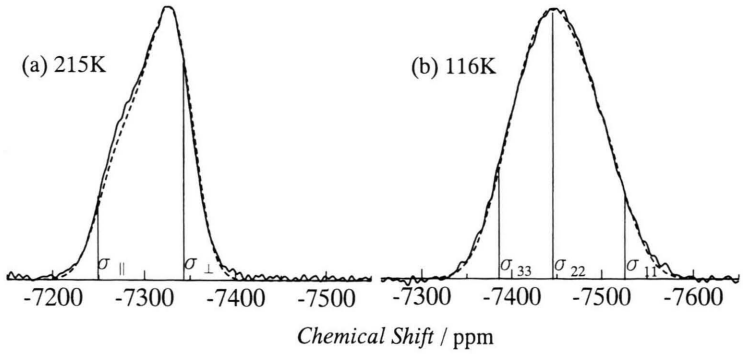

Fig. 4. ^{195}Pt NMR spectra of $[Cu(D_2O)_6][PtCl_6]$. The broken lines show the theoretical curves.

Table 1. Parameters obtained by the fitting calculation of ^{2}H NMR T_1.

$h^{-1}e^2Qq\sin(2\beta)$/kHz	τ_0/s	E_a/kJmol^{-1}	τ_{e0}/s	Δ/K
296	6×10^{-13}	15	9×10^{-11}	250

where γ_D is the gyromagnetic ratio of the ^{2}H nucleus, μ_B the Bohr magneton, g the g-value for Cu^{2+}, ω_e the angular ESR frequency and τ_e the correlation time of the electron spin. r_i is the distance between the ^{2}H nucleus and the i-th Cu^{2+} ion. $\omega_N \ll \tau_e^{-1} \ll \omega_e$ can be considered to hold in the 7.0 T magnetic field, and (12) can be rewritten as

$$T_{1P}^{-1} = \frac{2}{15}\gamma_D^2 g^2 \mu_B^2 \sum_i r_i^{-6} S(S+1)3\tau_e. \quad (13)$$

When τ_e is determined by the thermally activated transitions between the three different configurations caused by Jahn-Teller effect, τ_e can be written as

$$\tau_e = \tau_{e0}\exp(\Delta/kT), \quad (14)$$

where Δ is the activation energy for jumping between the different Jahn-Teller states. The least-squares fitting was performed by using equation

$$T_1^{-1} = T_{1Q}^{-1} + T_{1P}^{-1} \quad (15)$$

with $\hbar^{-1}e^2Qq\sin(2\beta)$, τ_0, E_a, τ_{e0}, and Δ as parameters. $\sum_i r_i^{-6}$ was obtained from the crystal data of $[Ni(H_2O)_6][SiF_6]$ [14], and the contribution from paramagnetic ions with 11^3 primitive cells around the resonant nucleus was calculated. The best-fit parameters are listed in Table 1. The obtained $\hbar^{-1}e^2Qq\sin(2\beta) = 296$ kHz was slightly larger than $\hbar^{-1}e^2Qq\sin(2\beta) = 230$ kHz calculated with $\beta = 55°$ and $e^2Qq/\hbar = 245$ kHz obtained by the lineshape simulation. This discrepancy can be considered to be due to omitting η from the calculation of T_{1Q} [20]. Converting τ_c to the jumping rate k with $k = (2\tau_c)^{-1}$, $k = k_0\exp(-E_a/RT)$ ($k_0 = 8\times10^{11}$ s^{-1}, $E_a = 15$ kJmol^{-1}) was obtained. Figure 3 shows the temperature dependence of k. Above the phase transition temperature, the obtained k_0 and E_a values can be considered to describe well the rate of 180° flips of the water molecules, since k estimated by these parameters agrees with those obtained from the spectral simulation. From this relatively small E_a value, it is predicted that the torsional oscillation about the bisector of the water molecule contributes largely to the temperature dependence of the e^2Qq/h value [15]. The τ_e value showed the order of 10^{-10} s from room temperature to the phase transition temperature. This result equals that obtained from ^{195}Pt NMR and ^{35}Cl NQR T_1 in the protonated compound [2, 3].

^{195}Pt NMR

^{195}Pt NMR spectra of $[Cu(D_2O)_6][PtCl_6]$ are shown in Figure 4. An H_2PtCl_6 solution was used for the standard sample of the chemical shift. The spectra showed the axially symmetric and unsymmetric powder pattern of the chemical shift anisotropy in the high and low temperature phase, respectively. The temperature dependences of the principal values of the chemical shift for $[Cu(H_2O)_6][PtCl_6]$ and $[Cu(D_2O)_6][PtCl_6]$ are shown in Figure 5. In the high temperature phase, the principal values decreased gradually with decreasing temperature. The perpendicular component of the principal values in the high temperature phase splitted into two components in the low temperature phase. For the parallel component of the principal values in the high temperature

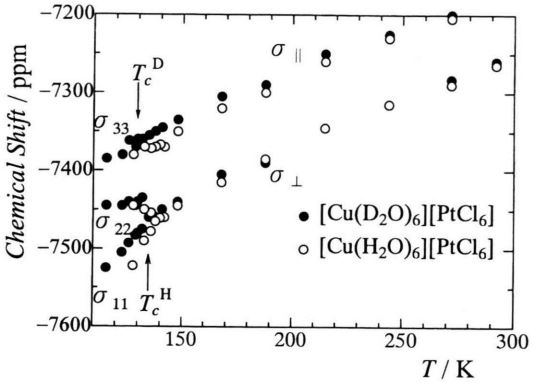

Fig. 5. Temperature dependence of the principal values of the anisotropic chemical shift of ^{195}Pt NMR in $[Cu(H_2O)_6][PtCl_6]$ and $[Cu(D_2O)_6][PtCl_6]$.

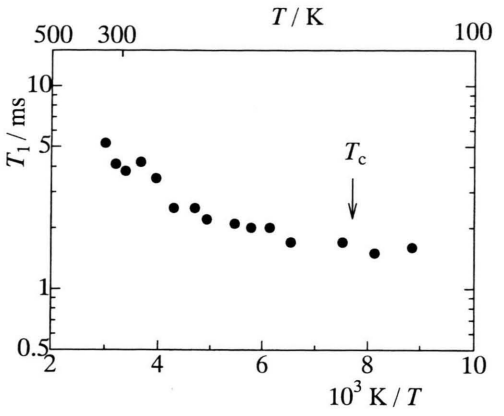

Fig. 6. Temperature dependence of ^{195}Pt NMR T_1 in $[Cu(D_2O)_6][PtCl_6]$.

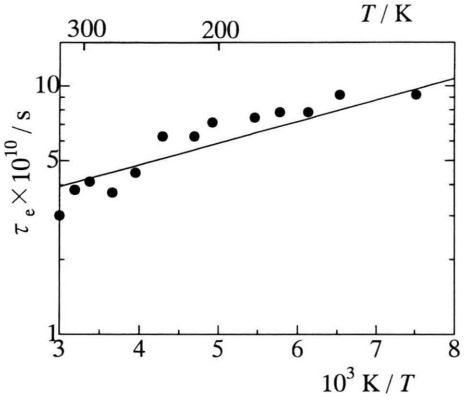

Fig. 7. Temperature dependence of τ_e obtained by ^{195}Pt NMR T_1 of $[Cu(D_2O)_6][PtCl_6]$.

phase, however, the drastic change around the transition could not be seen. A significant difference in the principal values between $[Cu(H_2O)_6][PtCl_6]$ and $[Cu(D_2O)_6][PtCl_6]$ was not observed. This phase transition, which is known as of first order, can be considered to be nearly second, since the principal values change continuously around the transition temperature [2].

Figure 6 shows the temperature dependence of ^{195}Pt T_1 of $[Cu(D_2O)_6][PtCl_6]$. T_1 can be considered to be determined by the magnetic dipolar interaction between the ^{195}Pt nuclei and the Cu^{2+} ions, since the temperature dependence of T_1 is similar to that the result of $[Cu(H_2O)_6][PtCl_6]$ [3]. In this case, T_1 can be connected with the electron spin correlation time τ_e by the equation [3, 18, 19]

$$T_1^{-1} = \frac{2}{15}\gamma_{Pt}^2 g^2 \mu_B^2 \sum_i r_i^{-6} S(S+1) 3\tau_e \qquad (16)$$

where, γ_{Pt} is the gyromagntic ratio of the ^{195}Pt nucleus, μ_B is the Bohr magneton, and g is g-value for Cu^{2+}. r_i is the distance between the ^{195}Pt nucleus and i-th Cu^{2+} ion.

$\sum_i r_i^{-6}$ was obtained from the crystal data of $[Cu(H_2O)_6][PtCl_6]$ [21, 22], and the contribution from paramagnetic ions with 11^3 primitive cells around the resonant nucleus was calculated [3]. The temperature dependence of τ_e, which was estimated from T_1, is shown in Figure 7. τ_e can be considered to be determined by the thermal jumping rate between the three Jahn-Teller distorted configurations of $[Cu(D_2O)_6]^{2+}$ above the transition temperature. By fitting the function $\tau_e = \tau_{e0}\exp(\Delta/kT)$ to the estimated temperature dependence of τ_e, a pre-exponential factor $\tau_{e0} = 1.0\times10^{-10}$ s and an activation energy Δ = 200 K (140 cm^{-1}) were obtained. The obtained Δ is smaller than that of the protonated compound [2, 3]. The height of the Jahn-Teller potential is predicted to be lowered by the deuteration, and this is consistent with the lower temperature shift of the phase transition for the deuterated compound.

[1] A. Sasane, H. Shinohara, Y. Mori, Y. Kume, T. Asaji, and D. Nakamura, Z. Naturforsch. **42a**, 611 (1987).
[2] M. Mizuno, T. Asaji, D. Nakamura, and K. Horiuchi, Z. Naturforsch. **45a**, 527 (1990).
[3] M. Mizuno, M. Suhara, T. Asaji, and Y. Furukawa, J. Mol. Struct. **345**, 123 (1995).
[4] F. S. Ham, Electron Paramagnetic Resonance, ed. by S. Geschwind, Plenum Press, New York 1972, p. 1.
[5] I. B. Bersuker, The Jahn-Teller Effect and Vibronic Interactions in Modern Chemistry, ed. by J. P. Fackler, Jr., Plenum Press, New York 1984.
[6] D. J. Siminovitch, M. Rance, K. R. Jeffrey, and M. F. Brown, J. Magn. Reson. **58**, 62 (1984).
[7] T.-H. Lin, J. A. DiNatale, and R. R. Vold, J. Amer. Chem. Soc. **116**, 2133 (1994).
[8] R. R. Vold, Nuclear Magnetic Resonance Probes of Molecular Dynamics, ed. by R. Tycko, Kluwer Academic Publishers 1994, p. 27.
[9] S. E. Woehler, R. J. Wittebort, S. M. Oh, D. N. Hendrickson, D. Inniss, and C. E. Strouse, J. Amer. Chem. Soc. **108**, 2938 (1986).
[10] S. E. Woehler, R. J. Wittebort, S. M. Oh, T. Kambara, D. N. Hendrickson, D. Inniss, and C. E. Strouse, J. Amer. Chem. Soc. **109**, 1063 (1987).
[11] S. M. Oh, S. R. Wilson, D. N. Hendrickson, S. E. Woehler, R. J. Wittebort, D. Inniss, and C. E. Strouse, J. Amer. Chem. Soc. **109**, 1073 (1987).
[12] M. S. Greenfield, A. D. Ronemus, R. L. Vold, R. R. Vold, P. D. Ellis, and T. E. Raidy, J. Magn. Reson. **72**, 89 (1987).
[13] M. E. Rose, Elementary Theory of Angular Momentum, Wiley, New York 1957.
[14] S. Ray, A. Zalkin, and D. H. Templeton, Acta Cryst. **B29**, 2741 (1973).
[15] T. Chiba and G. Soda, Bull. Chem. Soc. Japan **41**, 1524 (1968).
[16] D. A. Torchia and A. Szabo, J. Magn. Reson. **49**, 107 (1982).
[17] Y. Hiyama, J. V. Silverton, D. A. Torchia, J. T. Gerig, and S. J. Hammond, J. Amer. Chem. Soc. **108**, 2715 (1986).
[18] A. Birkeland and I. Svare, Phys. Scrip. **18**, 154 (1978).
[19] M. O. Norris, J. H. Strange, J. G. Powles, M. Rhodes, K. Marsden, and K. Krynicki, J. Phys. C 1, 422 (1968).
[20] R. R. Vold and R. L. Vold, Advances in MAGNETIC and OPTICAL RESONANCE, vol.16, ed. by W. S. Warren, Academic Press,Inc. 1991.
[21] L. Pauling, Z. Kristallogr. **72**, 482 (1930).
[22] Crystal Data Determinative Tables, 3rd ed., vol. 2: Inorganic Compounds, U.S. Department of Commerce, National Bureau of Standards, and the Joint Committee on Powder Diffraction Standards, USA, 1973.